



LASER DEPOSITION OF BRONZE ALUMINUM ON STEEL SUPPORT

Simona BOICIUC

„Dunarea de Jos” University of Galati

e-mail: simonaboiciuc@yahoo.com

ABSTRACT

In order to rise the wear and corrosion resistance of 0.45% C superficial steel layers, a multilayer coating was tested by injection of powder with 88.3% Cu; 9.5% Al; 2.2% Fe in melted bath by CO₂ continuous wave laser. Layers made by different laser conditions were characterized by macro and microstructure analysis, phase quality analysis, by X ray diffractometry and microhardness analysis. Research was carried out regarding the importance of nickel alloy intermediary layer for the rising of cladding quality.

KEYWORDS: laser cladding, aluminum bronzes, microstructure, microhardness, diffractometry.

1. Introduction

Biphase aluminum bronzes are known for their outstanding wear resistance, cavitation, corrosion etc., widely used in naval, petrochemical, chemical industry, etc. (bearings, rods, valve, pump impellers, and compressor screws and rotors, etc.).

Copper alloys with 9-11% Al feature, in addition to high corrosion resistance, good casting and hot forming properties and heat treatment hardening capacity of martensitic quenching and tempering.

According to the equilibrium diagram, Cu-Al alloys have balanced structure consisting of plastic solid solution α and eutectoid ($\alpha + \gamma_2$), where γ_2 is a solid hard and brittle solution based on the electronic Cu₃₂Al₁₉, compound.

Classical quenching consists of [1-3] heating at temperatures of 980-1000 °C in the β solid solution range based on the Cu₃Al, electronic compound, followed by rapid cooling in water. According to the thermal kinetic diagram, at higher cooling rates there is a diffusion transformation, with the solid solution ordering $\beta \rightarrow \beta_1$, after which the diffusion-free transformation of phase β_1 occurs in a needle-type martensite structure β' [1-3].

This structure has a relatively low hardness due to the coarse grain formed at high temperatures and in the presence of phase α . Subsequent tempering at 400-550 °C causes reverse transformations: $\beta' \rightarrow \beta_1$ and β_1 phase decomposition in a dispersed mixture $\alpha + \gamma_2$, having hardening effect.

Thus the CuAl10Fe4Ni4 alloy after quenching from 980 °C in water and tempering at 400 °C, increases its hardness from 170-200 HB to over 400 HB.

In the special Cu-Al alloys there are additions of Fe, Ni, Mn, which change the solubility of aluminum in copper and lead to new phases. Iron polishes granulation and improves mechanical and antifriction properties. In Fe-rich alloys an intermetallic compound FeAl₃ may occur with hardening and embrittlement effect. Nickel and manganese increase corrosion resistance and provide further hardening by solid solution alloying.

Laser heating has the advantage that it provides very fast heating rates (over 10³ °C/s) at high temperatures and similar cooling speed, which allows hardening of aluminum with bronze both in liquid and solid phases while maintaining an ultrafine granulation [4-8]. Laser surface quenching, however, has the disadvantage of relatively small thickness of the hardened layer, a certain variation of the properties of the hardened layer depth and the need for subsequent tempering [9-11].

Multilayer deposition of aluminum bronze powders injected onto the laser melted surface has the advantage of making thick layers with uniform chemical composition and properties throughout the section.

This paper presents laboratory experimental research on multilayer deposit on a steel support by injecting biphase aluminum bronze powders in a laser molten bath.

2. Experimental conditions

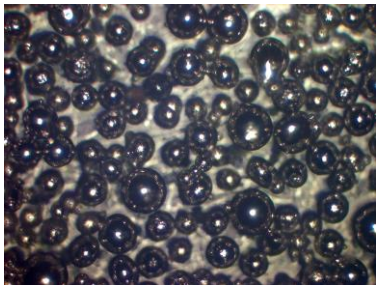
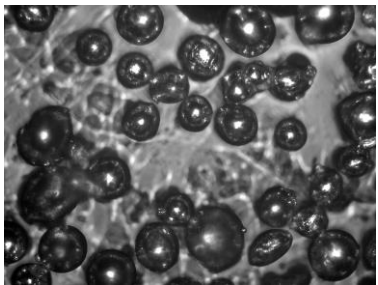
2.1. Sample preparation

For coating, use was made of a two-phase aluminum bronze powder, capable of hardening by quenching. Table 1 shows the origins, chemical composition and particle shape of the addition materials. The powder was aspherical, so that fluid

flowing on the surface of processed addition material was stimulated by vibration. Since the coating with aluminum bronze on the steel support indicated a low quality of the deposited layers geometry (rough surface, thin deposit and micro-cracks), its deposition on a buffer layer of nickel alloy was experienced and a very good deposition on steel substrate was found.

Coatings were made on samples of 25 x 25 x 15 mm of 0.45% C normalized carbon steel.

Table 1. Characteristics of the added materials used

Nr. crt.	Type of added material	Chemical composition of added material	Grain shape
1	Nickel alloy „Alliages Speciaux 7569 ALLIAGES FRITTÉS, Franța”.	8.9% Cr; 4.5% Fe; 5.1% B; 2.4% Al; 0.6% Cu; rest Ni.	
2	Bronze with alluminum „Rototec Proces FRIXTEC CASTOLIN U.S.A.”.	9.5% Al; 2.2% Fe; rest Cu.	

Laboratory experiments were conducted on a CO₂ continuous wave laser facility type GT with power of 1400 W, with coordinate table and computer for the process control, equipped with a powder injection system on the support surface.

Laboratory tests used a 1.8 mm diameter laser beam, which made partially overlapping parallel strips. The final thickness of the layer was achieved by superposition of five layers.

To determine the optimum deposition regime, the added material flow rate was varied, Q, from 53 to 150 mg/s, beam power, P, from 900 to 1200 W, surface scanning speed, v, from 5-7 mm/s and transverse movement step, p, 1 to 2 mm.

The nickel alloy buffer layer was deposited by the superposition of two layers, under the following conditions: Q = 53 mg/s, P = 1100 W, v = 7 mm/s, p = 1-2 mm. Table 2 shows the experimented working regimes and thickness, h, of the deposits obtained. Deposition regime was characterized by energy density factor $K = P / d * v$, which ranged within $79.3 \div 100 \text{ J/mm}^2$.

2.2. Structural properties

Initially deposited layers were characterized by macroscopic analysis of the surface layer deposited. Microstructural analysis was performed on samples cross-section, perpendicular to the direction of laser processing.

The microstructure of the samples was observed by optical microscopy Olympus BX 51M.

For the phase qualitative analysis of the surface layer deposited, use was made of the diffractometer DRON 3 with copper anti-cathode, monochromatic diffraction beam, U = 34 kV, I = 30 mA; F₁ = 2 mm; F₂ = 0.5mm; $\omega = 1^\circ/\text{min}$; $v_{\text{strip}} = 720 \text{ mm/h}$ for the diffraction angle variation within $2\theta = 20^\circ \dots 75^\circ$.

2.3. Microhardness depth profile measurement

It was determined the microhardness profile HV_{0,1} (0.98N load) over the depth of the deposited

layers. Microhardness depth profiling measurements were performed using a PMT-3 apparatus.

Vickers microhardness was calculated according to the SR EN ISO 6507-1:2002 standard. Results are presented as a mean of three measurements.

3. Results and discussions

3.1. Structural properties

Macroscopic analysis highlights the deposited layer surface quality, thickness and adhesion to the support.

The macrostructures of the laser deposition of aluminum bronze show a low adhesion to the carbon steel support, which can be explained by the poor metal link due to the low solubility of solid copper in iron.

The surface layer is rough (Fig. 1) and requires subsequent removal by machining of a relatively large layer. Inside the layers, solidification shrinkage cracks have appeared. The coating is hardened and made brittle by diffusion of iron from the base material into the added material and formation of the compound $FeAl_3$.

Table 2. Experimental conditions and deposited layer thickness

Sample code	Q [mg/s]	P [W]	v [mm/s]	K [J/mm ²]	P [mm]	h [mm]	Observations
Bronze aluminum deposition on steel support							
1	86	1000	7	79.36	2	0.38	C
2	86	1100	7	87.30	2	0.5	C
3	110	900	7	71.42	2	0.16-0.54	C, N
4	150	900	5	100.00	2	0.06-0.49	C, N, E
5	150	1100	7	87.30	2	0.13-1.00	C, N
6	119	1100	7	87.30	2	0.08-1.23	C, N
7	119	1200	7	95.24	2	0.14-1.21	C, N
Bronze aluminum deposition on steel support, with middle nickel alloy layer							
8	53	1100	7	87.30	2	0.47	-
9	53	1100	7	87.30	1.5	0.74	-
10	53	1100	7	87.30	1	0.64	-

Note: C-cracks; N-non uniformities of the layer thickness, E-exfoliation

From Table 2 and Figure 1, it can be seen that the non-uniform thickness of the layer deposited under the same conditions and the surface roughness increase with increasing the added material flow rate over 86 mg/s (sample code 2, 5 and 6). This is explained by the increased added material flow rate under the same conditions of laser processing, the molten bath temperature decreases by additional energy consumption for heating and melting the powder, which increases the viscosity of the molten added material. With lower laser beam powers and higher flow rates, there is insufficient melting of the support material and lack of adhesion of the deposited layers (sample code 4). With the same added material flow rate, the layer thickness increases with higher laser beam power, more pronounced at higher flow rates (sample code: 1 and 2, 4 and 5). These macroscopic observations indicate that the samples code 1...7 show no practical interest.

The decrease in the added material flow rate to 53 mg/s and the use of a buffer layer of nickel alloy, unlimitedly soluble as solid in both iron and copper, increased the adhesion to the steel support and to the

deposited layer. The layer quality was significantly improved as this becomes uniform, compact, without solidification shrinkage cracks and with practical applicability. Note that when using a 1.8 mm diameter laser beam on the surface being processed, the max. layer thickness is obtained on a step of the transverse movement of the 1.5 mm sample.

Figures 2 and 3 show the microstructure of the deposited layer for samples code 1 and 10. Good support adherence of the deposited layer is visible. At the fusion limit there are no compactness defects or inclusions of metal. When coating is directly performed on steel support, the presence of transverse cracks is initiated at the solidification surface (Fig. 2a), while by using the buffer layer of nickel alloy, the deposited layer is compact and crack-free (Fig. 3a).

The microstructure of the deposited layer results from melting and ultra-fast solidification of the added material, followed by a partial self-tempering in the overlapping area of the strip deposited i.e. sub-layer tempering when an additional layer is deposited.

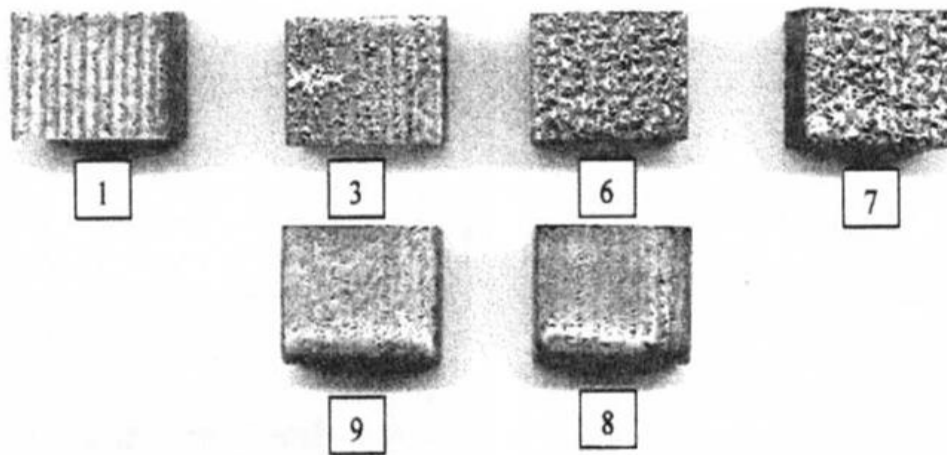


Fig 1. Macroscopic aspect of some thick bronze-aluminium samples

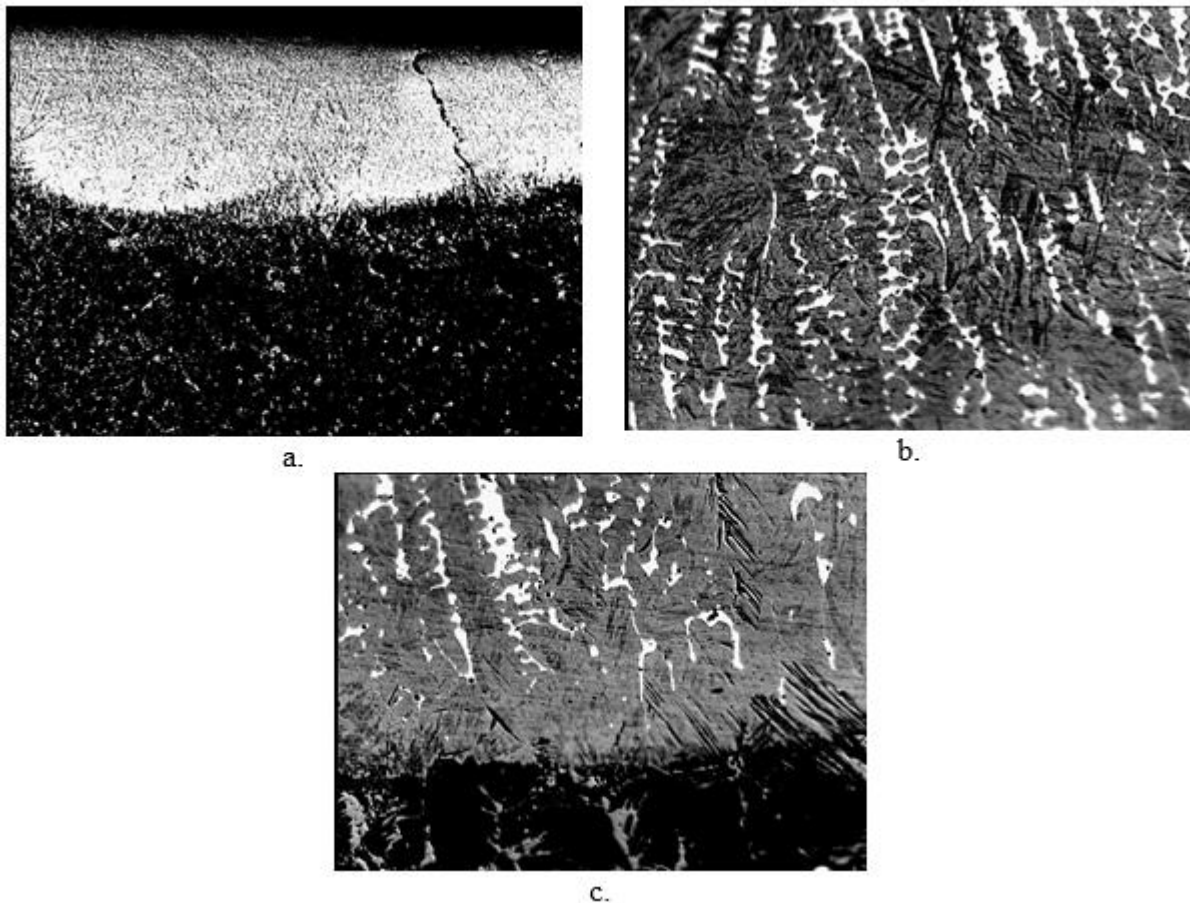


Fig. 2. Microstructure of the deposited layer with sample code 1 without Ni alloy middle layer a), general view x500; b). Middle of the deposited layer x1000; c). Base of the deposited layer x1000. Ferric chloride attack

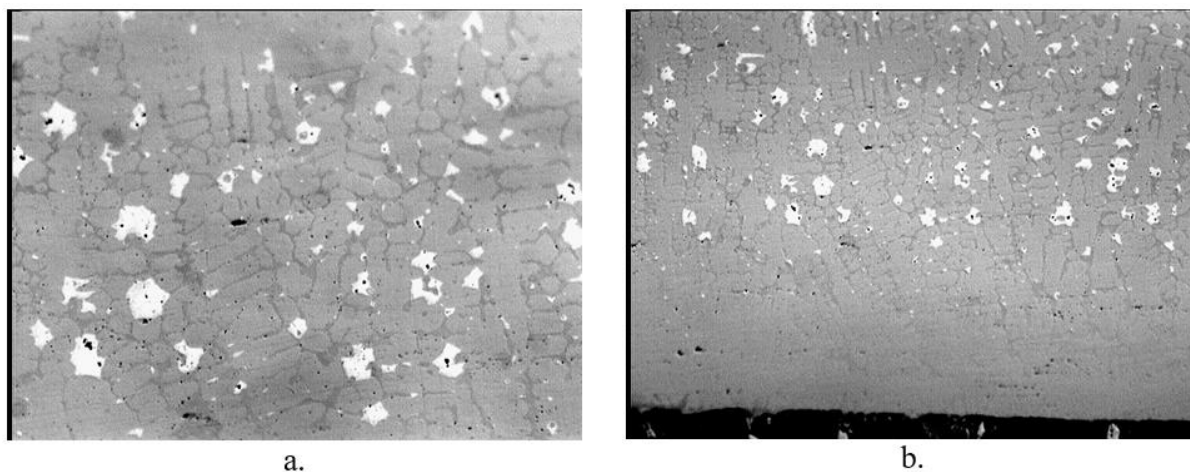


Fig. 3. Microstructure of the deposited layer with sample code 10 with Ni alloy middle layer a). Middle part of the deposited layer x1000; b). Base of the deposited layer x1000. Ferric chloride attack

For example, with sample code 1, the basic microstructure is fine columnar dendritic, at certain points with needle type appearance specific to hardening martensitic structures with coarse interdendritic separation of an intermetallic compound according to the diffraction diagram for the qualitative phase analysis of the deposited layers (Fig. 4). In the copper-based solid mass solution there is the interdendritically separated compound Fe - Al (Fig. 2b). The occurrence of relatively large quantities of compound is because the 2.2% Fe content in the added material is added to the iron by melting a steel substrate. Initiation and propagation of transverse shrinkage cracks upon solidification can be accounted for by the hard and brittle compound. At the base of the deposited layer there is a small thickness dilution

layer which makes the transition to the steel support with a small amount of Fe-Al compound. With the sample code 10, the microstructure is similar to a smaller amount of intermetallic compound – K - phase-intermetallic compound of Fe, Al, Ni (Fig. 5) with rosette aspect, because the layer of molten nickel alloy, which alloys the filler material, had a smaller amount of iron and the nickel presence slows the diffusion processes upon compound separation.

Additional nickel alloying of the added material led to a solid solution of copper, more resistant to metallographic attacks.

The unlimited solubility of copper and the nickel bases of the added material and buffer do not allow for the creation of a buffer zone separating the two deposits.

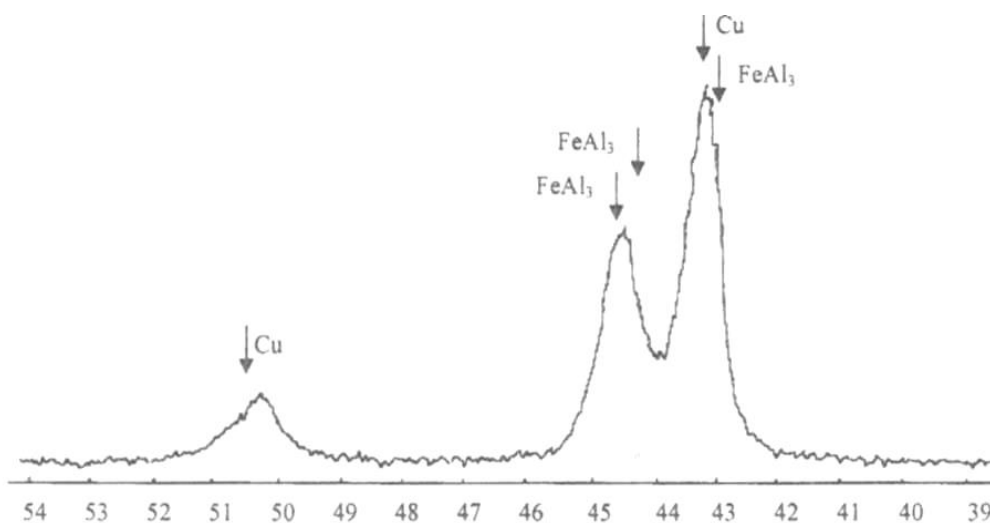


Fig. 4. Diffractogram for the layer clad for sample code 1

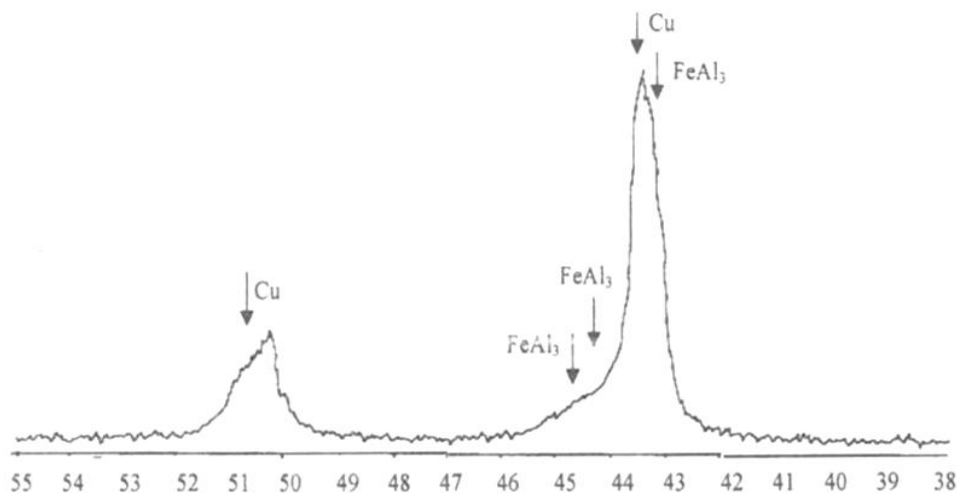


Fig. 5. Diffractogram for the layer clad for sample code 10

3.2. Microhardness depth profile measurement

Figure 6 shows the variation of microhardness HV0.1 over the depth of the layer deposited on the sample code 1 and 10. Microhardness maximum corresponds to a sample code 1, due to the presence of FeAl₃ compound in large amount and due to the

stability of the martensitic structure to the quick tempering process.

The layers obtained with nickel alloy buffer layer have less hardness because nickel reduces the amount of intermetallic compound and increases the amount of the additionally alloyed solid solution of copper. Microhardness is maximal in the buffer layer of the nickel alloy with higher thermal stability.

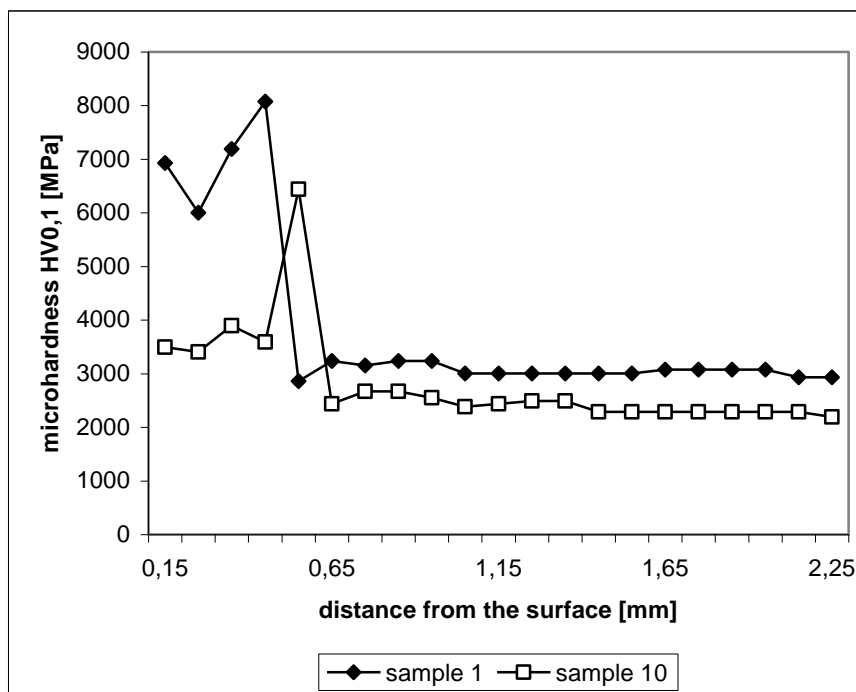


Fig. 6. Variation of microhardness HV0.1 over the depth of the layer deposited on the sample code 1 and 10

Comparing the microhardness of the multilayer deposit by laser with the properties of the aluminum

bronzes, laser hardened in the liquid phase and tempering [5-7], it was found that laser deposition

resulted in higher microhardness and greater depths. This is due to alloying bronze with nickel and iron, to the finer microstructure and the self-tempering process.

4. Conclusions

Multilayer deposition by aluminum bronze powder injection into the laser melted bath on steel base presents difficulties because of the poor adhesion of the deposit to the steel support, the non-uniformities of the deposited layer and shrinkage cracks. The coating is hardened and made brittle by diffusion of iron from the base material into the added material and by the formation of FeAl_3 compound.

Non-uniformity of the deposition increases with the deposit filler flow rate over 86 mg/s and lower laser beam power, below 1000 W.

Introducing a buffer layer of nickel alloy has improved adhesion, thickness uniformity and compactness of the aluminum bronze deposited layers. The optimum deposition regime was nickel alloy middle layer, regimes 9 and 10, which ensured a 0.64 to 0.74 mm thick layer with a microhardness HV0,1 ranging between 3895 and 3406 MPa.

Multilayer deposit ensures self-tempering of the layer and provides a superior microhardness at depths greater than the liquid phase quenching of aluminum bronzes of similar chemical composition.

References

- [1]. **Jan Lodewijk de Mol van Otterloo**, *Surface engineering with lasers*, Thesis, Shell Research and Technology Centre, Amsterdam, 1996.
- [2]. **Shi Z, Boyce A, Sun Y, Bell T.**, *Effect of Processing Parameters on Structure and Properties of Surface Melted Aluminum Bronze*, Eoromat, vol. E+D, p. 365-371, 1995.
- [3]. **Levcovici S. M., Levcovici D. T., Paraschiv M. M.**, *Laser Hardening of Aluminum Bronzes*, Materials and manufacturing processes, vol. 17, p. 13-22, 2002.
- [4]. **M. F. Schneider**, *Laser cladding with powder*, Ph. D. Thesis University of Twente, Enschede, Olanda, 1998.
- [5]. **H. Gedda**, *Laser surface cladding - a literature survey*, Lulea University of Technology, Division of Materials Processing, Suedia, 2000.
- [6]. **D. Salehi**, *Sensing and control of Nd:YAG laser cladding process*, Ph. D. Thesis, Swinburne University of Technology, Melbourne, Australia, 2005.
- [7]. **R. P. Martukanitz, S. S. Babu, J. M. Vitek**, *Development of Advanced Wear and Corrosion Resistant Systems through Laser Surface Alloying and Materials Simulation*, Applied Research Laboratory, State College, PA 16804, Oak Ridge National Laboratory.
- [8]. **F. Vollertsen, K. Partes, J. Meijer**, *State of the art of Laser Hardening and Cladding*, Proceedings of the Third International WLT – Conference on Lasers in Manufacturing, Munich, 2005.
- [9]. **S. Levcovici, D. T. Levcovici, C. Gheorghies, S. Boiciuc**, *Laser Cladding of Ni-Cr-B-Fe-Al Alloy on a Steel Support*, The International Thermal Spray Conference and Exposition (ITSC), 15-17 may, Seattle, USA, ISBN 0-87170-836-1.
- [10]. **S. Boiciuc, S. Levcovici, D. T. Levcovici, C. Gheorghies**, *Characterisation of hard coatings obtained by laser cladding process*, Metalurgia international, 9, p. 32-39, 2008.
- [11]. **S. Boiciuc, et al.**, *EDX Analysis of Laser Cladding Layers with Ni-Cr-B-Fe-Al Alloy*, Conference UgalMat, Galati, Romania, 2009.